

*Validation of goose liver fat measurement
by QCT and CSE-MRI with biochemical
extraction and pathology as reference*

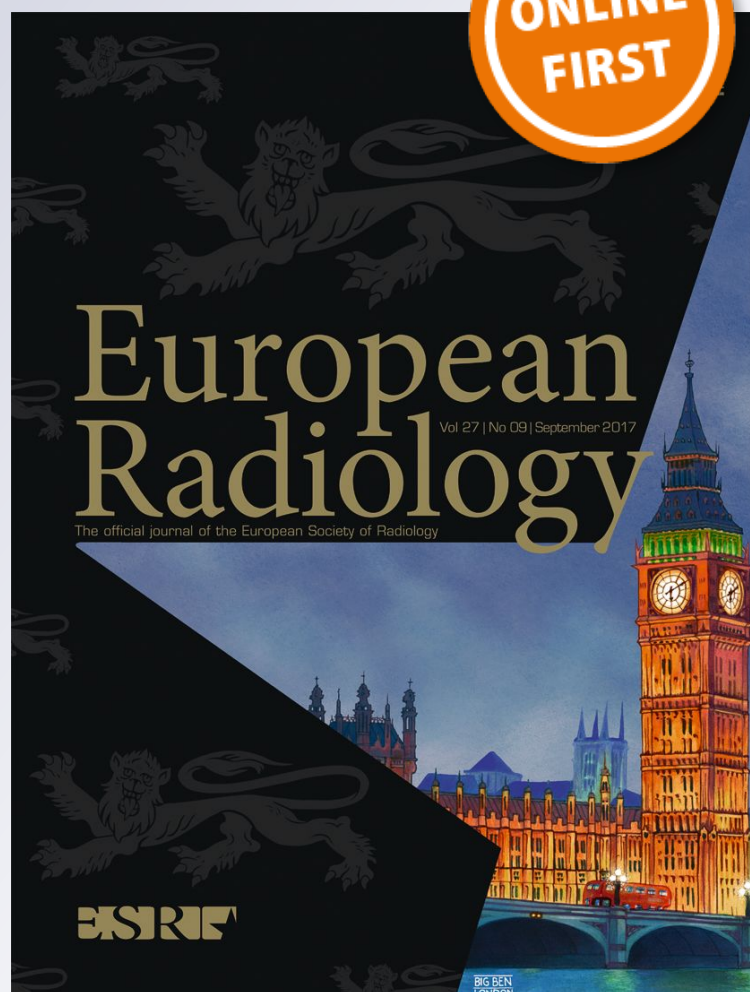
**Li Xu, Yangyang Duanmu, Glen
M. Blake, Chenxin Zhang, Yong Zhang,
Keenan Brown, Xiaoqi Wang, Peng
Wang, Xingang Zhou, Manling Zhang, et**

European Radiology

ISSN 0938-7994

Eur Radiol

DOI 10.1007/s00330-017-5189-x



Your article is protected by copyright and all rights are held exclusively by European Society of Radiology. This e-offprint is for personal use only and shall not be self-archived in electronic repositories. If you wish to self-archive your article, please use the accepted manuscript version for posting on your own website. You may further deposit the accepted manuscript version in any repository, provided it is only made publicly available 12 months after official publication or later and provided acknowledgement is given to the original source of publication and a link is inserted to the published article on Springer's website. The link must be accompanied by the following text: "The final publication is available at link.springer.com".



Validation of goose liver fat measurement by QCT and CSE-MRI with biochemical extraction and pathology as reference

Li Xu¹ · Yangyang Duanmu¹ · Glen M. Blake² · Chenxin Zhang¹ · Yong Zhang¹ · Keenan Brown³ · Xiaoqi Wang⁴ · Peng Wang⁵ · Xingang Zhou⁵ · Manling Zhang⁶ · Chao Wang⁷ · Zhe Guo¹ · Giuseppe Guglielmi⁸ · Xiaoguang Cheng¹

Received: 5 June 2017 / Revised: 5 November 2017 / Accepted: 9 November 2017
© European Society of Radiology 2017

Abstract

Objectives This study aimed to validate the accuracy and reliability of quantitative computed tomography (QCT) and chemical shift encoded magnetic resonance imaging (CSE-MRI) to assess hepatic steatosis.

Methods Twenty-two geese with a wide range of hepatic steatosis were collected. After QCT and CSE-MRI examinations, the liver of each goose was removed and samples were taken from the left lobe, upper and lower half of the right lobe for biochemical measurement and histology. Fat percentages by QCT and proton density fat fraction by MRI (MRI-PDF) were measured within the sample regions of biochemical measurement and histology. The accuracy of QCT and MR measurements were assessed through Spearman correlation coefficients (r) and Passing and Bablok regression equations using biochemical measurement as the "gold standard".

Results Both QCT and MRI correlated highly with chemical extraction [$r = 0.922$ ($p < 0.001$) and $r = 0.949$ ($p < 0.001$) respectively]. Chemically extracted triglyceride was accurately predicted by both QCT liver fat percentages ($Y = 0.6 + 0.866 \times X$) and by MRI-PDF ($Y = -1.8 + 0.773 \times X$).

Conclusions QCT and CSE-MRI measurements of goose liver fat were accurate and reliable compared with biochemical measurement.

Key Points

- QCT and CSE-MRI can measure liver fat content accurately and reliably
- Histological grading of hepatic steatosis has larger sampling variability
- QCT and CSE-MRI have potential in the clinical setting

Keywords Hepatic steatosis · Quantitative computed tomography · Chemical shift encoded magnetic resonance imaging · Proton density fat fraction · Hepatic triglyceride analysis

Abbreviations

NAFLD Non-Alcoholic Fatty Liver Disease
QCT Quantitative Computed Tomography
BMD Bone Mineral Density

pQCT peripheral Quantitative Computed Tomography
PDF Proton Density Fat Fraction
CSE-MRI Chemical Shift Encoded Magnetic Resonance Imaging
mDixon modified Dixon

✉ Xiaoguang Cheng
xiaog65@263.net

¹ Department of Radiology, Beijing Jishuitan Hospital, 31 Xijiekou East Street, Beijing 100035, China

² Biomedical Engineering Department, King's College London, London, UK

³ Mindways Software, Austin, TX, USA

⁴ Philips Healthcare, Beijing, China

⁵ Pathology Department, Capital Medical University Affiliated Beijing Ditan Hospital, Beijing, China

⁶ China National Food & Safety Supervision and Inspection Centre, Beijing, China

⁷ Statistics Department, Beijing Jishuitan Hospital, Beijing, China

⁸ Department of Radiology, Scientific Institute Hospital, San Giovanni Rotondo, Italy

Introduction

Non-alcoholic fatty liver disease (NAFLD) represents a spectrum of disorders characterised by the accumulation of fat in the liver [1, 2]. Worldwide, the prevalence of NAFLD ranges from 9 to 37% [1–4], and NAFLD is the most common aetiology of chronic liver disease in developed countries [5, 6]. Liver biopsy with semi-quantitative histological steatosis grading is the current reference standard for the diagnosis and grading of NAFLD [4, 7]. This method is invasive and unsuitable for screening large numbers of subjects at risk. Furthermore, biopsy suffers from high sampling variability [8, 9], and semi-quantitative grading of hepatic steatosis is strongly observer-dependent [10, 11].

Computed tomography (CT) evaluation of hepatic steatosis is based on the attenuation values of the liver parenchyma, evaluated as Hounsfield Units (HUs). Several quantitative CT indices, such as difference in attenuation between liver and spleen (CT_{L-S}), hepatic attenuation index (HAI) and the ratio of hepatic attenuation to splenic attenuation ($CT_{L/S}$), have been used to assess hepatic steatosis [12–15]. However, the observed spleen average CT value may vary with factors, and this makes the above-mentioned CT indices inconsistent across different subjects. Quantitative CT (QCT) was originally developed for the measurement of bone mineral density (BMD) of the spine [16]. After vigorous quality control, a calibration phantom is scanned simultaneously with the subject, which makes it possible to interpret the CT HU of tissue in terms of a physical density [17]. The QCT phantom includes standards representative of fat and water, making it possible to infer the fat content of a tissue from its CT HU and increasing adiposity is associated with a decrease in HU [18]. QCT greatly reduces the impact of the sources of variability across CT scanners and patients, such as kVp, X-ray filtration, patient size and the variation of CT HU of spleen. Peripheral QCT (pQCT) was found to have good accuracy and precision for determining percent body fat and liver fat in small animals [19]. The measurement of liver fat content using QCT with a clinical CT scanner has not yet been reported. Neither has the validation of fat evaluation by QCT using chemical extraction techniques or histology been previously described, whereas such validation is essential before the technique is applied clinically.

With its ability to detect a very low quantity of fat, proton magnetic resonance spectroscopy ($^1\text{H-MRS}$) is widely accepted to assess hepatic steatosis [20–22]. However, MRS is not routinely used because it is time-consuming, and samples only a small portion [23]. In recent years, several techniques of quantitative magnetic resonance imaging (MRI) have been introduced for fast acquisition of quantitative proton density fat fraction (PDFF) maps covering large parts of the liver or

the entire organ [24–27]. Chemical shift encoded MRI (CSE-MRI) can discriminate between fat and water spins based on their different resonance frequencies, and its multi-echo variants such as modified Dixon techniques (mDixon) permit flexible times to echo (TE) not restricted to exact in-phase/opposed-phase values. Multi-echo CSE-MRI techniques with the corrections for $T2^*$ decay and inclusion of multi-peak spectral models has been validated with excellent correlation with $^1\text{H-MRS}$ and histological methods [28–32]. However, only limited validation studies including both CT and CSE-MRI have been reported for the determination of hepatic fat content [33, 34].

The purpose of the present study was to validate the quantification of liver fat content by QCT and CSE-MRI PDFF on a group of geese with a wide range of hepatic steatosis, using biochemical extracted triglyceride as the reference.

Materials and methods

Experimental procedures

Experimental animals

A total of 22 Landes geese from the Jinjiang goose breeding farm (Linq, Shandong, China) were selected. All geese were given a normal diet until 2 months old, and then were overfed with 250–350 g corn at an interval of 6 h each day for 0–28 days. All geese received humane care according to the *Guide for the Care and Use of Laboratory Animals* by the National Academy of Sciences and published by the National Institutes of Health (NIH publication 86-23, revised 1985).

Quantification of liver fat content by QCT

QCT was performed using a Toshiba Aquilion 80-slice CT scanner (Toshiba, Tokyo, Japan) with a Mindways calibration phantom (Mindways Software, Austin, TX, USA) placed beneath each goose. During the scan, the feet and wings of the goose were taped and no anaesthetic was used. Scan parameters were 0.985 pitch, 120 cm table height, 120 kV, 125 mA, 1.0 mm thickness, 500 mm² field of view (FOV), standard reconstruction. The scan range included 2 cm above the diaphragm to 15 cm below the diaphragm. Images were then analysed using Mindways QCT PRO three-dimensional (3D) spine module software version 4.2.

On the 3D reconstructed images an elliptical cylinder ROI (thickness of 9 mm and area of 180–220 mm²) was individually placed in the centre part of the left lobe, upper [right-superior (RS)], and lower [right-inferior (RI)] half of right lobe, the QCT-derived bone mineral density (BMD_{Sample}), BMD calibration slope and field uniformity correction (FUC) were exported. According to the calculation formula

provided by Mindways, the percent fat by volume of goose liver (β) was obtained [18].

All QCT ROI measurements were performed by one trained radiologist (with 2 years of experience of QCT measurement), blinded to the general information of the samples and MRI results. The intra-observer agreement of QCT measurements was evaluated for all samples by the same observer in duplicate analyses performed 1 month apart.

Quantification of liver fat content by MRI-PDFF

At the same day as the QCT examination, all the geese were slaughtered and then underwent an MR scan on a clinical 3-T whole-body MRI system (Ingenia 3.0 T; Philips Healthcare, Best, The Netherlands) with a 32-channel dS Torso Body coil. A six-echo mDixon-quant gradient-echo sequence (CSE-MRI implementation) was acquired and the parameters employed were: flip angle = 3°, time of repetition (TR) = 8.1 ms, first TE (TE1) = 1.33 ms, TE shift (Δ TE) = 1.3 ms, FOV = 220 × 178 × 90 mm³, voxel size = 1.5 × 1.54 × 3 mm³, number of signals acquired (NSA) = 4. Thirty axial slices were reconstructed with a voxel size of 1.38 mm and matrix of 160. A T2-weighted turbo spin echo (TSE) coronal sequence was also acquired and the parameters were: TR = 488 ms, TE = 60 ms, slice thickness = 5 mm, slice gap = 1 mm, FOV = 220 × 182 mm², voxel size = 0.55 × 0.65 mm², NSA = 2.

The image data were processed with the ISP software (Version 7; Philips Healthcare, Best, The Netherlands). PDFF maps were generated by accounting for all known confounding factors, such as seven-peak fat spectrum modelling [29], bias from T1 and noise [35], T2* correction [36] and novel eddy current compensation [29, 35–37]. Detailed algorithm for the mDixon-quant hepatic fat fraction is given in a previous publication [30]. One trained radiologist (with 1 year of experience of MRI-PDFF measurement) performed the MR scan and measurements, blinded to the general information of the samples and QCT results. The axial PDFF map images representing the middle part of the three lobes were selected using the coronal TSE image as a reference, and ROIs were placed with the position and size as same as on QCT. The intra-observer agreement of MRI-PDFF measurements was assessed using two ROI measurements by the same radiologist with an interval of 1 month.

Sampling of goose liver

Immediately after the MR scan, each goose was dissected, and the whole liver was removed and weighed. The left and right lobes of the liver were separated, and the right lobe was cut into upper and lower halves. Samples (sized 60×30×30 mm) were taken from the middle of the left, RS and RI lobes. A

small piece of tissue was taken from each sample and fixed in formalin immediately for pathology exam. The samples were kept refrigerated (4 °C) before sending to the lab for biochemical measurement.

Quantification of lipid content of liver by biochemical analysis

The chemical measurement was performed in the National Food & Safety Supervision and Inspection Centre with Soxhlet extraction [38]. The 66 liver tissue samples were dried to constant weight (103 ± 2 °C), and then weighed. Triglyceride content (g) of the dry samples were determined by biochemical extraction. The triglyceride mass percent of the goose liver were obtained using the triglyceride content (g) and the wet weight (g) of the sample. The volume of fat mass and fat-free tissue of goose liver was calculated with the equation $V = m / \rho$, and the triglyceride volume percent of the goose livers were then obtained [$\beta = 100 \times V_{Fat} / (V_{Fat} + V_{Fat-free})$]. The value of density of fat mass (ρ_{Fat}) is 0.9007 g/cm³ [39], and the density of the fat-free tissue of goose liver ($\rho_{Fat-free}$) was 1.18 g/cm³ using the mean value of three randomly selected liver samples.

Histological grading of liver steatosis

A total of 61 specimens were obtained and stained with haematoxylin and eosin, and five liver tissue samples were destroyed. The histological results were interpreted by a hepatopathologist who was blinded to the general information of the samples and imaging results. The percentage of cells affected by fat vacuoles was separated by grade: grade 0 for less than 5%, grade 1 for 5–30%, grade 2 for 31–50%, grade 3 for 51–75% and grade 4 for more than 75% [40].

Statistical analyses

All statistical analyses and graphs were conducted by a statistician using SAS (Version 9.3; SAS Institute, Cary, NC, USA). The intra-observer agreements of imaging measurements were calculated using Bland-Altman 95% limits of agreement analyses as well as intra-class correlation coefficients. Passing and Bablok regression equations were calculated between imaging measurements and biochemical extraction. Spearman correlation coefficients (r) were computed to express the degree of linear association between measures. We defined correlation coefficients as strong if $r > 0.8$ and excellent if $r > 0.9$. To detect the variability of fat distribution, we compare the values of the three ROIs derived from the same goose liver, using mixed model repeated measurements analysis. Data were considered significant when $p < 0.05$.

Results

Characteristics of samples obtained

The weight of the sample livers ($n = 22$) ranged from 0.088 to 0.778 kg. Gross visual evaluation demonstrated the wide range of hepatic steatosis of the geese livers (Fig. 1a). These differences of hepatic steatosis were clearly observed by QCT (Fig. 1b), MRI-PDFF (Fig. 1c) and histology (Fig. 1d). Overall, the mean value [\pm standard deviation (SD), range] of biochemical triglyceride mass percentage, biochemical triglyceride volume percentage, fat percentage by QCT (Fat%_{QCT}) and MRI-PDFF was 24.13% (\pm 21.1%, 0.04–58.7%), 25.2% (\pm 21.87%, 0.04–60.54%), 28.21% (\pm 25.67%, -2.19–69.07%) and 33.81% (\pm 27.53%, 0.88–79.41%), respectively (Fig. 2).

Intra-observer agreements of QCT and MRI-PDFF measurement

Bland-Altman analyses demonstrated a very high intra-observer agreement for both QCT and MRI-PDFF ROI measurements (Fig. 3). The intra-class correlation coefficient was 0.997 ($p < 0.001$) for QCT ROI measurement and 0.998 ($p < 0.001$) for MRI-PDFF ROI measurement.

Accuracy of QCT and MRI-PDFF measurement

A high correlation was detected between Fat%_{QCT} and triglyceride volume percentage, as well as between MRI-PDFF and triglyceride mass percentage, with Spearman correlation coefficients of $r = 0.922$ ($p < 0.001$) and $r = 0.949$ ($p < 0.001$), respectively. Passing and Bablok regression indicated that triglyceride volume percentage can be predicted by Fat%_{QCT} (Fig. 4a), and triglyceride mass percentage can be predicted by MRI-PDFF (Fig. 4b).

In comparison to biochemical extraction, both QCT and MRI-PDFF significantly overestimated liver fat content. The mean value of difference between Fat%_{QCT} and triglyceride volume percentage was 3.0% [95% confidence interval (95%CI), -8.33 to 14.33%; $p < 0.001$], and the mean value of difference between MRI-PDFF and triglyceride mass percentage was 9.68% (95%CI, -5.28 to 24.63%; $p < 0.001$).

Histological results compared to biochemical extraction and imaging modalities

Figure 5 shows the distribution of triglyceride volume percentage, Fat%_{QCT} and MRI-PDFF at each division of histological grading. The biochemical result of each group defined by histology was 0.04–6.95% for grade 0, 2.69–7.09% for grade 1, 5.08–9.86% for grade 2, 11.39–25.85% for grade 3 and 10.2–60.54% for grade 4, respectively (Fig. 5a). The

Fig. 1 Samples of geese livers with different amount of fat content, ranging from healthy liver to liver with severe steatosis. **a** Photographs demonstrate increased size and yellow hue with increasing steatosis (left to right). **b** QCT enabled volumetric quantification of steatosis within the centre part of RS lobe (samples 1, 2 and 4) and RI lobe (sample 3), and the results of samples 1, 2, 3 and 4 was 2.83%, 4.18%, 24.26% and 435.25%, respectively. **c** MRI-PDFF map detected fat fraction of samples 1, 2, 3 and 4 was 2.78%, 12.75%, 34.73%, and 43.08%, respectively. The size and position of ROIs by MRI-PDFF were as same as QCT. **d** Histological grade was grade 0, grade 2, grade 3 and grade 4, respectively. Triglyceride mass percentage by chemical extraction was 0.25%, 9.2%, 23.36%, and 33.84%, respectively

results of QCT and MRI-PDFF of each histologically graded group were -2.19 to 6.89% and 2.78–10.4% for grade 0, 0.17–3.0% and 4.18–16.78% for grade 1, 1.11–4.18% and 6.45–12.75% for grade 2, 11.62–24.26% and 13.04–36.92% for grade 3, and 12.55–69.07% and 12.09–79.41% for grade 4, respectively (Fig. 5b and c).

Variability of fat distribution

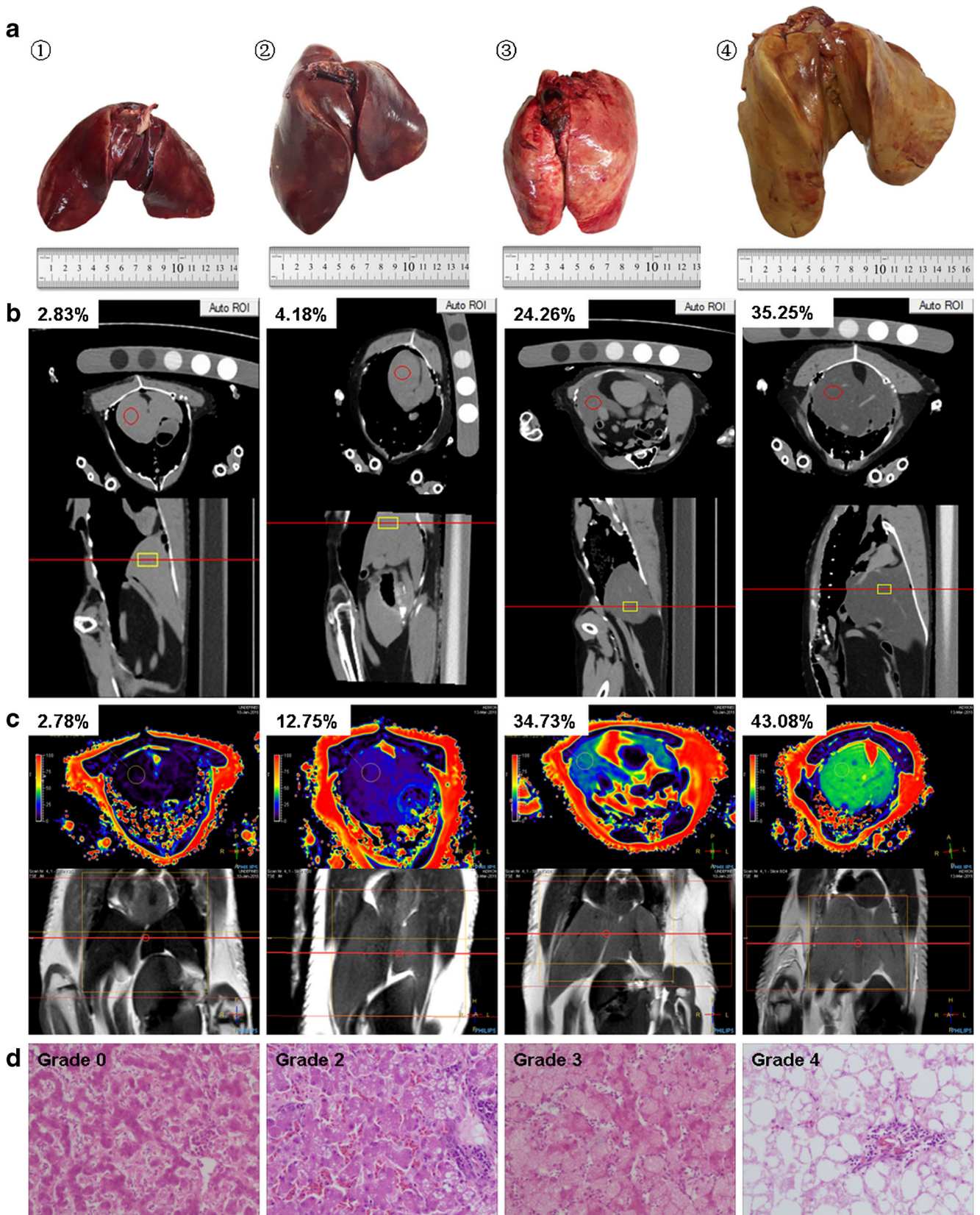
No statistically significant differences of fat percentage among the three sampled regions of goose liver were detected by QCT ($p = 0.993$), MRI-PDFF ($p = 0.995$), biochemical extraction ($p = 0.998$) or histological grading ($p = 0.416$).

Discussion

The present study evaluated the fat content of goose liver using QCT and CSE-MRIPDFF and validated these measurements against biochemically extracted triglyceride percent as reference. The findings from this study impact on the clinical management of steatosis.

In principle, QCT measures the fat fraction averaged by volume, and CSE-MR imaging PDFF measures the number of hydrogen protons in fat compared to the number in both fat and water. Therefore, we compared QCT measurements with triglyceride volume percentage and MRI-PDFF with triglyceride mass percentage. Both QCT and MRI-PDFF measurements were found to have very high intra-observer agreements, and considering the minor variability of fat distribution among the three sample regions, both techniques had negligible ROI sampling errors. Furthermore, we found excellent correlations between biochemical extraction and QCT as well as with MRI-PDFF. In terms of the accuracy of QCT and MRI-PDFF, the differences between the two imaging modalities and the "gold standard" were small. Compared to the two imaging modalities, histological grading of liver steatosis had greater ROI sampling errors and more obvious disagreement with biochemical extraction.

Nagy and Johnson reported the use of pQCT to measure liver fat in 26 female lemmings and found that pQCT had good precision [mean intra-individual coefficients of variation



(CV) = 0.3%] for determining percent liver fat, and there was a high correlation ($r = -0.98, p < 0.01$) between the attenuation values of liver by pQCT and chemically extracted triglyceride [19]. According to the validation study of CT on animals (24 mice) conducted by Lubura et al. [41] the correlation between the liver fat content by micro-CT {liver fat (%) = [Spleen (HU) – Liver (HU)] / [Spleen (HU) – Fat (HU)]} and biochemically extracted triglyceride was high ($r^2 = 0.915$), with a regression slope of 1.7. Artz et al. [33] reported an in vivo validation of dual-energy CT on a group of obese mice for quantification of hepatic steatosis, and CT attenuation was found highly correlated with both biochemically extracted triglyceride ($r^2 = 0.89$) and MRI-PDFF ($r^2 = 0.86$). In a study on a group of obese patients using non-contrasted CT, Shores et al. [42] demonstrated high correlation of $CT_{L/S}$ ($r = -0.80, p < 0.001$) as well as $CT_{L/S}$ ($r = -0.80, p < 0.001$) with chemically measured triglyceride using needle and wedge liver biopsy. Compared to previous studies, we demonstrated that QCT provided a direct value of volume percent of liver fat that had an excellent correlation with triglyceride by biochemical extraction. Moreover, the slope (0.87) and intercept (0.6%) of the regression between QCT and biochemical extraction indicated the high accuracy of QCT to quantify liver fat content.

A concern for using CT in routine liver fat assessment is the radiation exposure involved. For a QCT study, the exposure can be half of a routine liver scan without affecting the accuracy of measurement, and limiting the number of slices acquired can further reduce the radiation dose [43]. In the

clinical setting, a QCT scan can be incorporated with a routine clinical CT scan, and liver fat content and visceral fat area [44] can be obtained with a single CT scan without additional radiation.

In previous studies, the correlation coefficient between MRI measured liver fat content and chemically estimated liver fat varied from 0.74 to 0.96 [33, 45–48]. Runge et al. [45] reported a study comparing CSE-MRI (using a four-echo mDixon technique with a single fat peak reconstruction) to biochemical triglyceride in a group of mice. The slope and intercept of the linear regression between MRI measured liver fat content and liver triglyceride content was 0.045 and 1.6, respectively [45]. In the study by Hijona et al. [46] the slope and intercept of the linear regression between MRI fat fraction and liver triglyceride content was 0.0253 and -0.0482, respectively [46]. Hines et al. [47], conducted a validation study of CSE-MRI in a group of obese mice compared to lipid extraction, and in their study, a linear relationship was shown between the MRI-PDFF (reconstructed with multi-peak spectral models and with T2* correction) and lipid extraction (slope, 1.11; intercept, -6.3%) Compared to those previous studies, our study demonstrated comparable results regarding to the correlation coefficient between MRI and biochemical extraction (0.949 vs 0.74–0.96). Considering the different algorithms of MR data among different studies, the disagreements of the slope and intercept of linear regression equations are not unexpected. MRI-PDFF was also detected with a similar correlation coefficient with biochemical extracted triglyceride content compared to CT both in the study by Artz et al. [33] ($r^2 = 0.92$ vs $r^2 = 0.89$) and in our study ($r = 0.95$ vs $r = 0.92$). These results again justified that CSE-MRI PDFF could be a method of choice for human liver steatosis assessment.

The MR mDixon-quant technique is complicated and the results can be influenced by many factors. First, MRI-PDFF measures the ratio of number of hydrogen protons in fat comparing to the number in both fat and water, while biochemical extraction measures the triglyceride content in the liver. Another issue is that mDixon MRI (using relatively longer TE than in solid state physics spectroscopy methods) cannot measure the signal from hydrogen protons that are closely connected to large proteins, or in a solid or semi-solid state. The “dry” mass of tissue could account for 3–15% of total mass. These factors generate a systematic shift in the final output, and may explain the relative larger difference between MRI-PDFF and biochemical extraction observed in this study compared to that between QCT and biochemical extraction.

The present study demonstrated that histological grade poorly reflected the severity of goose liver steatosis. Due to its invasive nature, sampling error, and incapability to repeat the measurement at the same site, histology seems to be less favourable to assess and monitor change of liver fat content in comparison to QCT and MRI-PDFF.

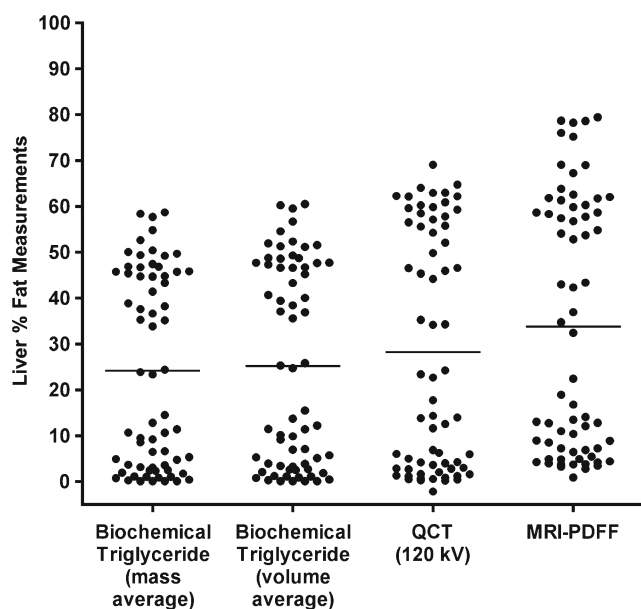


Fig. 2 Plots of liver fat percentage measured by chemical extraction (mass and volume averages), QCT, and MRI. The mean value of biochemical triglyceride mass percentage, biochemical triglyceride volume percentage, fat percentage by QCT and MRI-PDFF was 24.13%, 25.2%, 28.21%, and 33.81%, respectively

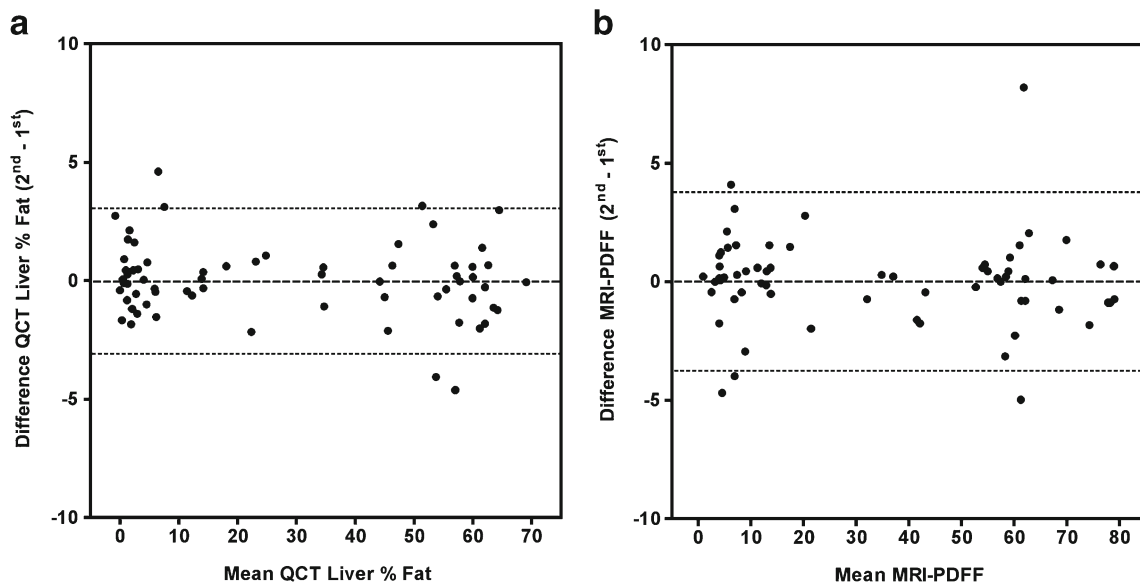


Fig. 3 Bland-Altman analyses of intra-observer agreement for repeated ROI measurements. **a** QCT showed a very high intra-observer agreement, mean difference between the two ROI measurements by the same observer was -0.005% (95% limits of agreement, -3.10 to 3.09%, $p = 0.999$). **b**

MRI-PDFF showed a similarly high intra-observer agreement as QCT, mean difference between the two ROI measurements by the same observer was 0.05% (95% limits of agreement, -3.73 to 3.82%, $p = 0.991$)

There are several limitations to our study. (1) Even though every effort was made to match the ROIs of the QCT and MRI measurements to the chemical and histology samples, exact matching was impossible, and this may result in some differences. However, our data also showed that there was little variation among the sample regions, which indicated that steatosis was homogenous within the liver. (2) Geese were killed before MR scan, and therefore the alteration of blood perfusion may

bias the MRI signal. The potential influence of blood perfusion on the MRI signal should be addressed in a future study.

In conclusion, both QCT and CSE-MRI methods can measure liver fat content accurately and reliably in comparison with chemical methods, and these results justify the use of QCT and CSE-MRI in the clinical setting to assess and monitor liver steatosis, but further validations are needed on patients and community populations.

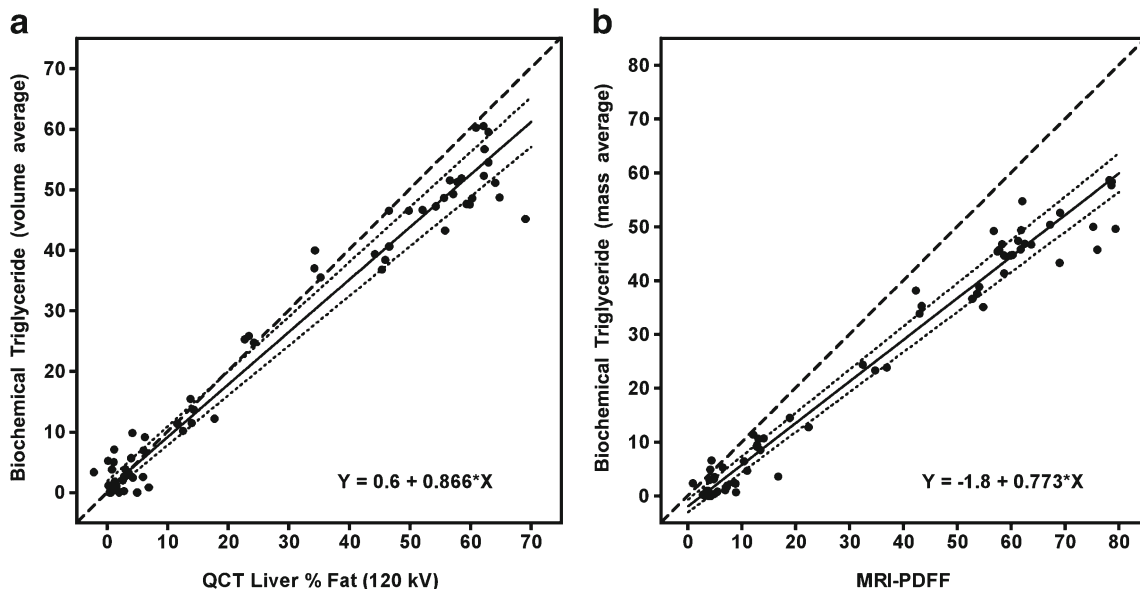


Fig. 4 Passing and Bablok regression of biochemical extraction with QCT and MRI. **a** QCT determined fat percentage is able to predict biochemical triglyceride volume percentage with the

equation: $Y = 0.6 + 0.866 \times X$ ($r = 0.922$). **b** MRI-PDFF can predict biochemical triglyceride mass percentage with the equation: $Y = -1.8 + 0.773 \times X$ ($r = 0.949$)

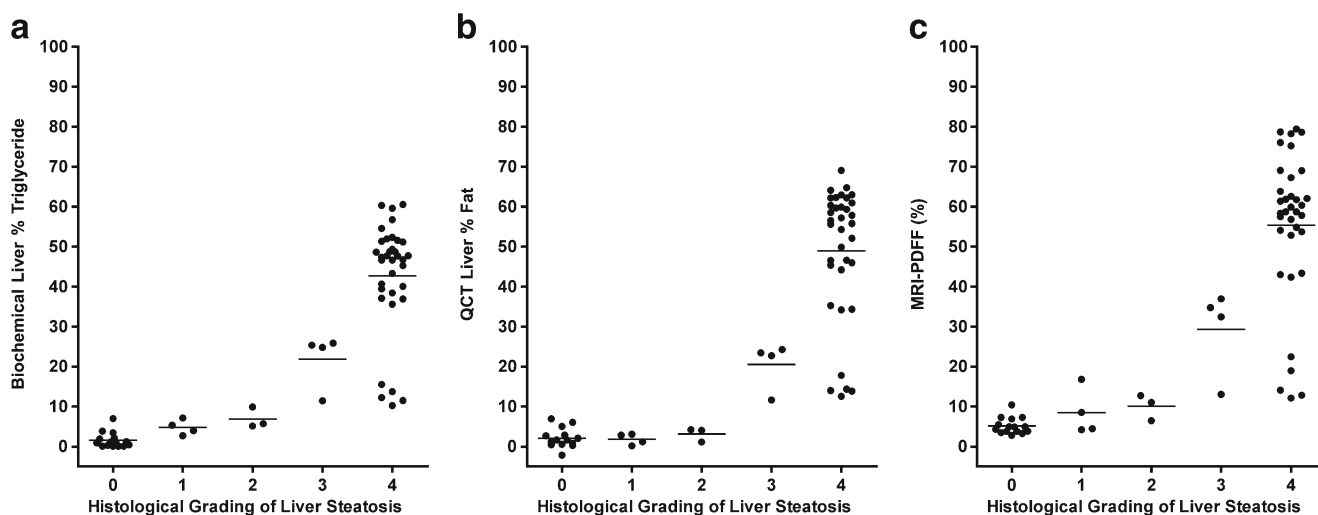


Fig. 5 Plots of biochemical triglyceride volume percentage, QCT determined fat percentage and MRI-PDFF grouped by histological grading. **a** The mean chemical result of each group defined by histology was 1.55% for grade 0, 4.75% for grade 1, 6.88% for grade 2, 21.83% for grade 3 and 42.72% for grade 4, respectively. **b** The mean result by QCT

was 2.02% for grade 0, 1.78% for grade 1, 3.1% for grade 2, 20.50% for grade 3 and 48.93% for grade 4, respectively. **c** The mean value of MRI-PDFF was 5.12% for grade 0, 8.46% for grade 1, 10.06% for grade 2, 29.29% for grade 3 and 55.34% for grade 4, respectively

Acknowledgements We thank our study participants for contributing with their time and efforts. We wish to thank Mindways Software and Philips Healthcare for their technical support. We also thank Chao Wang for his professional suggestions on statistics. The authors acknowledge the support of National Natural Science Foundation of China (81401407).

Funding: This study has received funding by National Natural Science Foundation of China (81401407).

Compliance with ethical standards

Guarantor The scientific guarantor of this publication is Li Xu.

Conflict of interest The authors of this manuscript declare relationships with the following companies. Keenan Brown is the employee and stock owner of Mindways Software. There was no involvement by this company in the design, execution, analysis, or publication of this manuscript. Xiaoqi Wang is employed by Philips Healthcare. There was no involvement by this company in the design, execution, analysis, or publication of this manuscript. All the other authors declare no potential conflict of interest.

Statistics and biometry Chao Wang kindly provided statistical advice for this manuscript.

One of the authors has significant statistical expertise.

Ethical approval Institutional Review Board approval was obtained.

Approval from the institutional animal care committee of Beijing Jishuitan Hospital was obtained.

Methodology

- prospective
- diagnostic or prognostic study
- performed at one institution

References

1. Bedogni G, Miglioli L, Masutti F, Tiribelli C, Marchesini G, Bellentani S (2005) Prevalence of and risk factors for nonalcoholic fatty liver disease: the Dionysos nutrition and liver study. *Hepatology* 42:44–52
2. Vernon G, Baranova A, Younossi ZM (2011) Systematic review: the epidemiology and natural history of non-alcoholic fatty liver disease and non-alcoholic steatohepatitis in adults. *Aliment Pharmacol Ther* 34:274–285
3. Williams CD, Stengel J, Asike MI, Torres DM, Shaw J, Contreras M, Landt CL et al (2011) Prevalence of nonalcoholic fatty liver disease and nonalcoholic steatohepatitis among a largely middle-aged population utilizing ultrasound and liver biopsy: a prospective study. *Gastroenterology* 140:124–131
4. Chalasani N, Younossi Z, Lavine JE, Diehl AM, Brunt EM, Cusi K, Charlton M et al (2012) The diagnosis and management of non-alcoholic fatty liver disease: practice Guideline by the American Association for the Study of Liver Diseases, American College of Gastroenterology, and the American Gastroenterological Association. *Hepatology* 55:2005–2023
5. Ong JP, Younossi ZM (2007) Epidemiology and natural history of NAFLD and NASH. *Clin Liver Dis* 11:1–16
6. Sass DA, Chang P, Chopra KB (2005) Nonalcoholic fatty liver disease: a clinical review. *Dig Dis Sci* 50:171–180
7. Brunt EM, Janney CG, Di Bisceglie AM, Neuschwander-Tetri BA, Bacon BR (1999) Nonalcoholic steatohepatitis: a proposal for grading and staging the histological. *Am J Gastroenterol* 94:2467–2474
8. Ratziu V, Charlotte F, Heurtier A, Gombert S, Giral P, Bruckert E, Grimaldi A et al (2005) Sampling variability of liver biopsy in nonalcoholic fatty liver disease. *Gastroenterology* 128:1898–1906
9. Bedossa P, Dargere D, Paradis V (2003) Sampling variability of liver fibrosis in chronic hepatitis C. *Hepatology* 38:1449–1457
10. El-Badry AM, Breitenstein S, Jochum W, Washington K, Paradis V, Rubbia-Brandt L, Puhan MA et al (2009) Assessment of hepatic steatosis by expert pathologists: the end of a gold standard. *Ann Surg* 250:691–697

11. Kleiner DE, Brunt EM, Van Natta M, Behling C, Contos MJ, Cummings OW, Ferrell LD et al (2005) Design and validation of a histological scoring system for nonalcoholic fatty liver disease. *Hepatology* 41:1313–1321
12. Lee SS, Park SH (2014) Radiologic evaluation of nonalcoholic fatty liver disease. *World J Gastroenterol* 20:7392–7402
13. Lee SS, Park SH, Kim HJ, Kim SY, Kim MY, Kim DY, Suh DJ et al (2010) Non-invasive assessment of hepatic steatosis: prospective comparison of the accuracy of imaging examinations. *J Hepatol* 52:579–585
14. Park SH, Kim PN, Kim KW, Lee SW, Yoon SE, Park SW, Ha HK et al (2006) Macrovesicular hepatic steatosis in living liver donors: use of CT for quantitative and qualitative assessment. *Radiology* 239:105–112
15. Park YS, Park SH, Lee SS, Kim DY, Shin YM, Lee W, Lee SG et al (2011) Biopsy-proven nonsteatotic liver in adults: estimation of reference range for difference in attenuation between the liver and the spleen at nonenhanced CT. *Radiology* 258:760–766
16. Cann CE, Genant HK (1980) Precise measurement of vertebral mineral content using computed tomography. *J Comput Assist Tomogr* 4:493–500
17. Kalender WA, Felsenberg D, Genant HK, Fischer M, Dequeker J, Reeve J (1995) The European spine phantom—a tool for standardization and quality control in spine bone mineral measurements by DXA and QCT. *Eur J Radiol* 20:83–92
18. Cheng XG, Blake GM, Brown JK, Guo Z, Zhou J, Wang FZ, Yang LQ et al (2017) The measurement of liver fat from single-energy quantitative computed tomography scans. *Quant Imaging Med Surg* 7:281–291
19. Nagy TR, Johnson MS (2004) Measurement of body and liver fat in small animals using peripheral quantitative computed tomography. *Int J Body Compos Res* 1:155–160
20. Bohte AE, Van Werven JR, Bipat S, Stoker J (2011) The diagnostic accuracy of US, CT, MRI and 1H-MRS for the evaluation of hepatic steatosis compared with liver biopsy: a meta-analysis. *Eur Radiol* 21:87–97
21. Reeder SB, Cruite I, Hamilton G, Sirlin CB (2011) Quantitative assessment of liver fat with magnetic resonance imaging and spectroscopy. *J Magn Reson Imaging* 34:729–749
22. Banerjee R, Pavlides M, Tunnicliffe EM, Piechnik SK, Sarania N, Philips R, Collier JD et al (2014) Multiparametric magnetic resonance for the non-invasive diagnosis of liver disease. *J Hepatol* 60:69–77
23. Pereira K, Salsamendi J, Casillas J (2015) The global nonalcoholic fatty liver disease epidemic: what a radiologist needs to know. *J Clin Imaging Sci* 5:32
24. Berglund J, Ahlstrom H, Johansson L, Kullberg J (2011) Two-point Dixon method with flexible echo times. *Magn Reson Med* 65:994–1004
25. Eggers H, Brendel B, Duijndam A, Herigault G (2011) Dual-echo Dixon imaging with flexible choice of echo times. *Magn Reson Med* 65:96–107
26. Idilman IS, Aniktar H, Idilman R, Kabacam G, Savas B, Elhan A, Celik A et al (2013) Hepatic steatosis: quantification by proton density fat fraction with MR imaging versus liver biopsy. *Radiology* 267:767–775
27. Reeder SB (2013) Emerging quantitative magnetic resonance imaging biomarkers of hepatic steatosis. *Hepatology* 58:1877–1880
28. Eggers H, Perkins TG, Hussain SM (2011) Influence of spectral model and signal decay on hepatic fat fraction measurements at 3 T with dual-echo Dixon imaging. *Proc Int Soc Magn Reson Med* 19:573
29. Yu H, Shimakawa A, McKenzie CA, Brodsky E, Brittain JH, Reeder SB (2008) Multiecho water-fat separation and simultaneous R2* estimation with multifrequency fat spectrum modeling. *Magn Reson Med* 60:1122–1134
30. Kukuk GM, Hittatiya K, Sprinkart AM, Eggers H, Gieseke J, Block W, Moeller P et al (2015) Comparison between modified Dixon MRI techniques, MR spectroscopic relaxometry, and different histologic quantification methods in the assessment of hepatic steatosis. *Eur Radiol* 25:2869–2879
31. Noble JJ, Keevil SF, Totman J, Charles-Edwards GD (2014) In vitro and in vivo comparison of two-, three- and four-point Dixon techniques for clinical intramuscular fat quantification at 3 T. *Br J Radiol* 87:20130761
32. Livingstone RS, Begovatz P, Kahl S, Nowotny B, Strassburger K, Giani G, Bunke J et al (2014) Initial clinical application of modified Dixon with flexible echo times: hepatic and pancreatic fat assessments in comparison with (1)H MRS. *Magn Reson Mater Phys* 27:397–405
33. Artz NS, Hines CDG, Brunner ST, Agni RM, Kuhn JP, Roldan-Alzate A, Chen GH et al (2012) Quantification of hepatic steatosis with dual-energy computed tomography: Comparison with tissue reference standards and quantitative magnetic resonance imaging in the ob/ob mouse. *Invest Radiol* 47:603–610
34. Kramer H, Pickhardt PJ, Kliever MA, Hernando D, Chen GH, Zagzebski JA, Reeder SB (2017) Accuracy of liver fat quantification with advanced CT, MRI, and Ultrasound techniques: prospective comparison with MR spectroscopy. *AJR Am J Roentgenol* 208:92–100
35. Liu CY, McKenzie CA, Yu H, Brittain JH, Reeder SB (2007) Fat quantification with IDEAL gradient echo imaging: correction of bias from T(1) and noise. *Magn Reson Med* 58:354–364
36. Yu H, McKenzie CA, Shimakawa A, Vu AT, Brau AC, Beatty PJ, Pineda AR et al (2007) Multiecho reconstruction for simultaneous water-fat decomposition and T2* estimation. *J Magn Reson Imaging* 26:1153–1161
37. Lu W, Yu H, Shimakawa A, Alley M, Reeder SB, Hargreaves BA (2008) Water-fat separation with bipolar multiecho sequences. *Magn Reson Med* 60:198–209
38. Wu CS, He JH, Guo XD, Luo HY, Ye JR, Huang JF, Wu YL et al (2008) Meat and meat products—determination of total fat content (GB/T 9695.7-2008). General Administration of Quality Supervision, Inspection and Quarantine of the People's Republic of China, Beijing, pp 1–3
39. Heymsfield SB, Lohman TG, Wang ZM, Going SB (2005) Human body composition, 2nd edn. Human Kinetics Publishers, Champaign Appendix
40. Schwimmer JB, Behling C, Newbury R, Deutsch R, Nievergelt C, Schork NJ, Lavine JE (2005) Histopathology of pediatric nonalcoholic fatty liver disease. *Hepatology* 42:641–649
41. Lubura M, Hesse D, Neumann N, Scherneck S, Wiedmer P, Schurmann A (2012) Non-invasive quantification of white and brown adipose tissues and liver fat content by computed tomography in mice. *PLoS One* 7:e37026
42. Shores NJ, Link K, Fernandez A, Geisinger KR, Davis M, Nguyen T, Sawyer J et al (2011) Non-contrasted computed tomography for the accurate measurement of liver steatosis in obese patients. *Dig Dis Sci* 56:2145–2151
43. Wang Y, Guo Z, Li D, Zhao HZ, Liu QH, Yu AH, Zhao YW et al (2012) Low-dose radiation in lumbar bone mineral density measurement by QCT. *Chin J Osteoporos* 18:992–995
44. Wang L, Wang W, Xu L, Cheng XG, Ma YM, Liu D, Guo Z et al (2013) Relation of visceral and subcutaneous adipose tissue to bone mineral density in Chinese women. *Int J Endocrinol* 2013:378632
45. Runge JH, Bakker PJ, Gaemers IC, Verheij J, Hakvoort TB, Ottenhoff R, Nederveen AJ et al (2014) Measuring liver triglyceride content in mice: non-invasive magnetic resonance methods as an alternative to histopathology. *MAGMA* 27:317–327
46. Hijona E, Sanchez-Gonzalez J, Alustiza JM, Hijona L, Arenas J, Garcia E, Rojas N et al (2012) Accurate fat fraction quantification by multiecho gradient-recalled-echo magnetic resonance at 1.5 T in rats with nonalcoholic fatty liver disease. *Eur J Radiol* 81:1122–1127

-
47. Hines CDG, Yu HZ, Shimakawa A, McKenzie CA, Warner TF, Brittain JH, Reeder SB (2010) Quantification of hepatic steatosis with 3T MR imaging: Validation in ob/ob mice. *Radiology* 254: 119–128
 48. Bannas P, Kramer H, Hernando D, Agni R, Cunningham AM, Mandal R, Motosugi U et al (2015) Quantitative MR imaging of hepatic steatosis: validation in ex vivo human livers. *Hepatology* 62:1444–1455